J Nanopart Res (2012) 14:804
DOI 10.1007/s11051-012-0804-x

RESEARCH PAPER

Vertically aligned ZnO–$ZnGa_2O_4$ core–shell nanowires: from synthesis to optical properties

Miao Zhong · Yanbo Li · Takero Tokizono · Maojun Zheng · Ichiro Yamada · Jean-Jacques Delaunay

Received: 4 August 2011 / Accepted: 26 February 2012 / Published online: 24 March 2012

Abstract Dense and vertically aligned ZnO–$ZnGa_2O_4$ core–shell nanowires were synthesized in large scale on *a*-plane sapphire substrates by a simple two-step chemical vapor deposition method. The synthesized ZnO–$ZnGa_2O_4$ core–shell nanowires were connected through their base by a thick underlayer of the same material realizing electrical contact of the nanostructured array. X-ray diffraction and transmission electron microscopy analyses of the core–shell nanowires reveal that the ZnO cores and $ZnGa_2O_4$ shells of the core–shell nanowires are of single-crystal quality and have aligned crystallographic orientations. The ultraviolet–visible diffuse reflectance spectra of the core–shell nanowires showed two sharp edges corresponding to near-band-edge absorption contributed by the ZnO cores and the $ZnGa_2O_4$ shells. Moreover, the room-temperature photoluminescence spectra of the core–shell nanowires gave three UV emission peaks coming from the $ZnGa_2O_4$ shells and the ZnO cores. The dense and vertically aligned ZnO–$ZnGa_2O_4$ core–shell nanowires showing promising photoelectric properties offer an ideal structure for light harvesting applications such as a photoanode in a photoelectrochemical water splitting cell.

Keywords Core–shell nanowires · Vertically aligned nanowires · Photoanode material · ZnO · $ZnGa_2O_4$

Electronic supplementary material The online version of this article (doi:10.1007/s11051-012-0804-x) contains supplementary material, which is available to authorized users.

M. Zhong (✉) · Y. Li · T. Tokizono · I. Yamada · J.-J. Delaunay (✉)
Department of Mechanical Engineering, The University of Tokyo, 7-3-1 Hongo, Bunkyo-ku, Tokyo 113-8656, Japan
e-mail: miaozhong@lelab.t.u-tokyo.ac.jp

J.-J. Delaunay
e-mail: jean@mech.t.u-tokyo.ac.jp

M. Zheng
Laboratory of Condensed Matter Spectroscopy and Opto-Electronic Physics, Department of Physics, Shanghai Jiao Tong University, Shanghai 200240, People's Republic of China

Introduction

Self-assembly of well-aligned one-dimensional semiconductor core–shell nanowires (NWs) has been actively researched in the past decade for their wide range of applications (Lauhon et al. 2002; Bakkers et al. 2004; Thelander et al. 2006; Li et al. 2006; Fan et al. 2006; Du et al. 2009; Cao et al. 2011). Compared to single-material NWs, the composite core–shell NWs can take advantage of each material and compensate for their individual shortcomings to satisfy the application requirements. Furthermore, the core–shell NWs can offer new functionalities, such as broad-range light sensitivity, prolonged carrier lifetime, and efficient

charge separation (Wang et al. 2008; Shu et al. 2009; Huang et al. 2009). These added functionalities are vital for the development of high-performance energy devices such as photoelectrochemical water splitting cells. For example, surface coating of photocatalyst shells on semiconductor NW cores improves the efficiency and stability when used as a photoanode material in a photoelectrochemical water splitting cell (Huang et al. 2009; Zhong et al. 2012). In this case, the semiconductor NW cores increase the light absorption and electrical conductivity, the photocatalyst shells improve surface photoreaction and anti-corrosive property, and the composite core–shell structures enhance the charge separation. However, the search of suitable semiconductor and photocatalyst materials to realize this functional core–shell NW structure with single-crystal quality remains a major issue.

$ZnGa_2O_4$ (ZGO), a wide band-gap semiconductor, has been investigated for its possible use in the overall water splitting under ultraviolet (UV) light radiation owing to the photocatalytic activity of its metal ions with a d^{10} electronic configuration (Ikarashi et al. 2002). Recently, visible-light-sensitive water splitting using Rh-doped ZGO powder has been reported (Kumagai et al. 2011). In that study, ZGO works as a host material to tune the energy band structure of $ZnRh_2O_4$ within its forbidden band to satisfy the requirements of visible-light water splitting reaction. Moreover, ZGO can be used as a precursor material for the synthesis of $Ga_{(1-x)}Zn_xN_{(1-x)}O_x$ solid-solution NWs (Han et al. 2010). The oxynitride solid-solution material is regarded as a promising photocatalyst for overall water splitting with solar light radiation (Maeda et al. 2005). Therefore, ZGO is a promising starting material for photocatalytic water splitting applications and structuring ZGO into a well-oriented nano-geometry could further improve the water splitting performance. However, a controllable synthesis of well-aligned single-crystal ZGO nanostructures in high density is still challenging. In contrast, ZnO can form dense and well-aligned NW structures in many fabrication processes (Fan et al. 2009), and the synthesized ZnO NW samples are good templates to support a radial growth of other functional materials forming well-aligned core–shell NW structures.

In this paper, dense and vertically aligned ZnO–ZGO core–shell NWs were fabricated in large scale by a simple two-step chemical vapor deposition (CVD) method. The roots of the core–shell NWs were connected through a thick underlayer of the same material realizing electrical contact of the core–shell NW layer. This structure is ideal for the use as a photoanode in a water splitting cell. A model was proposed to explain the growth mechanism of the ZnO–ZGO core–shell NWs. Moreover, ultraviolet–visible (UV–VIS) diffuse reflectance spectra and photoluminescence (PL) spectra of the ZnO–ZGO core–shell NWs were investigated to understand the energy band structures and the optical properties of the ZnO–ZGO core–shell NWs.

Experimental

Large-scale vertically aligned ZnO–ZGO core–shell NWs were prepared by a two-step CVD process. A schematic of the growth process is shown in Fig. 1. First, an *a*-plane sapphire was cleaned with acetone in a supersonic bath, and then the sapphire was coated with a discontinuous gold layer (1 nm in thickness) through a metal shadow mask. The Au-coated sapphire was then used as a substrate in the first-step CVD growth process. The Au-coated sapphire substrate was placed at the center of a furnace tube. Mixed powder of ZnO and graphite (2:1 in weight) was loaded in an alumina boat as precursors and the alumina boat was then placed 1 cm upstream of the sapphire substrate. Oxygen and argon gases were used as carrier gases (5:1 in volume ratio) at a working pressure of 50 mbar. The furnace was operated for 30 min at a temperature of 1,000 °C, and then cooled down to room

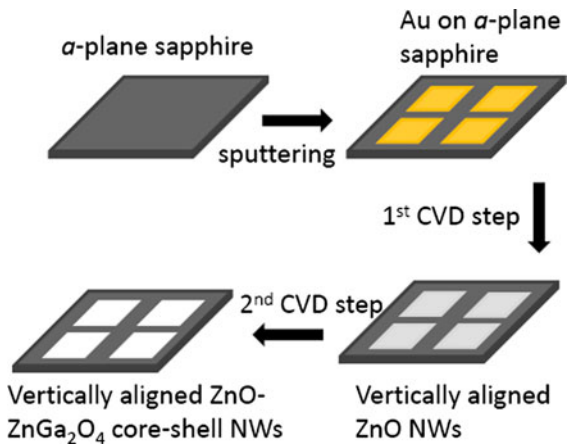

Fig. 1 The growth process of vertically aligned ZnO–$ZnGa_2O_4$ core–shell nanowires

temperature naturally. After this process, vertically aligned ZnO NWs were grown on the Au-coated surfaces of the *a*-plane sapphire substrate. The as-grown ZnO NWs sample was then used as a template in the second CVD growth process. The ZnO NW substrate was placed at a temperature position of 900 °C in the furnace tube. Mixed powder of Ga_2O_3, ZnO, and graphite was used as precursors, and was placed 11 cm upstream of the ZnO NW substrate. The temperature of the precursors was set to 1,180 °C. Argon and oxygen (10:1 in volume ratio) was used as carrier gases. After a 30 min growth process, vertically aligned ZnO–ZGO core–shell NWs were obtained in large scale on the substrate.

Scanning electron microscopy (SEM) images of the prepared NW samples were taken with a Hitachi S3000 N SEM equipment. X-ray diffraction (XRD) patterns of the prepared NW samples were obtained with a diffractometer (Miniflex II-MW, Rigaku Co. Ltd., Japan) using the CuKα radiation. Transmission electron microscopy (TEM) images and selected area electron diffraction (SAED) patterns of the prepared ZnO–ZGO NWs were obtained with a JEM 2010 equipment. The UV–VIS diffuse reflectance spectra of the NW samples were measured with a spectrophotometer (DRS, V-560, Jasco). The PL spectra of the NW samples were measured with a fluorescence spectrometer (FP-6600, JASCO) under an excitation wavelength of 325 nm.

Results and discussions

Figure 2a shows a typical SEM image of the vertical ZnO NWs. The NWs are well-aligned in large scale and have a uniform diameter of 75 nm and an average length of 5 μm. A high-resolution SEM image of Fig. 2b shows that the sidewalls of the ZnO NWs are straight and smooth. Figure 2c–f shows the SEM images of three types of ZnO–ZGO core–shell NWs grown under different conditions as listed in Table 1. The initial vertical alignment of the ZnO NWs was largely maintained after the formation of core–shell nanostructures. Figure 2c, d shows the SEM images of large-scale vertically aligned ZnO–ZGO core–shell NWs grown under the ZGO-1 condition. The average diameter of the NWs increases to about 90 nm. Figure 2e, f shows large-scale chain-like ZnO–ZGO core–shell NWs grown under the ZGO-2 condition. The core–shell NWs are formed by a compact stacking of ZGO nanocrystals on the ZnO NW cores. The average NW diameter is estimated to increase to about 130 nm, but have non-uniform shell surfaces in contrast to the previous case. Figure 2g, h shows the images of large-scale vertically aligned ZnO–ZGO core–shell NWs fabricated under the ZGO-3 condition. The average diameter of NWs is about 160 nm. The EDX analysis shows that the atomic ratios of Zn/Ga/O on the side edge of NWs were about 14/28/58 ($\sim$1/2/4), indicating the formation of ZGO NW shells. A tilted-angle SEM image of Fig. 2h shows that all NWs are straightly aligned but have non-uniform shell surfaces, bonded together at their roots and grown in a high density.

XRD measurements were taken to characterize the as-prepared samples of ZnO NWs and ZnO–ZGO core–shell NWs. Figure 3a shows a typical XRD pattern of the vertically aligned ZnO NWs after the first-step CVD growth. Only two sharp diffraction peaks indexed to the hexagonal ZnO (0002) and (0004) were observed. This is strong evidence for the alignment of the ZnO NWs along the [0001] direction. Figure 3b–d shows the XRD patterns of the ZnO–ZGO core–shell NWs fabricated under the three different growth conditions. Only four diffraction peaks indexed to the hexagonal ZnO (0002) and (0004), and the spinel ZGO (111) and (222) were observed. This result is strong evidence for the formation of ZGO shell layers with an aligned orientation along the ZGO [111] direction.

TEM and SAED analyses were further carried out to examine the crystal quality and the crystallographic orientations of the ZnO core and the ZGO shell of the core–shell NWs. The bright-field TEM image of Fig. 4 shows a straight NW with a core–shell structure grown under the ZGO-1 condition. The diameter of the NW core is about 70 nm, which is consistent with the diameter of 75 nm of the ZnO NWs synthesized in the first CVD growth step. The overall diameter of core–shell NW is about 90 nm from the TEM image, which is in agreement with the core–shell NW diameter of $\sim$90 nm shown in Fig. 2d. The SAED pattern of the shell region A (inset A) shows that the shell of the NW consists of a single-crystalline spinel ZGO layer with a [111] oriented crystal direction parallel to the long-axial direction of the NW. The calculated interplane spacing between the two close spots along the long-axial direction in the SAED pattern A is $\sim$0.48 nm,

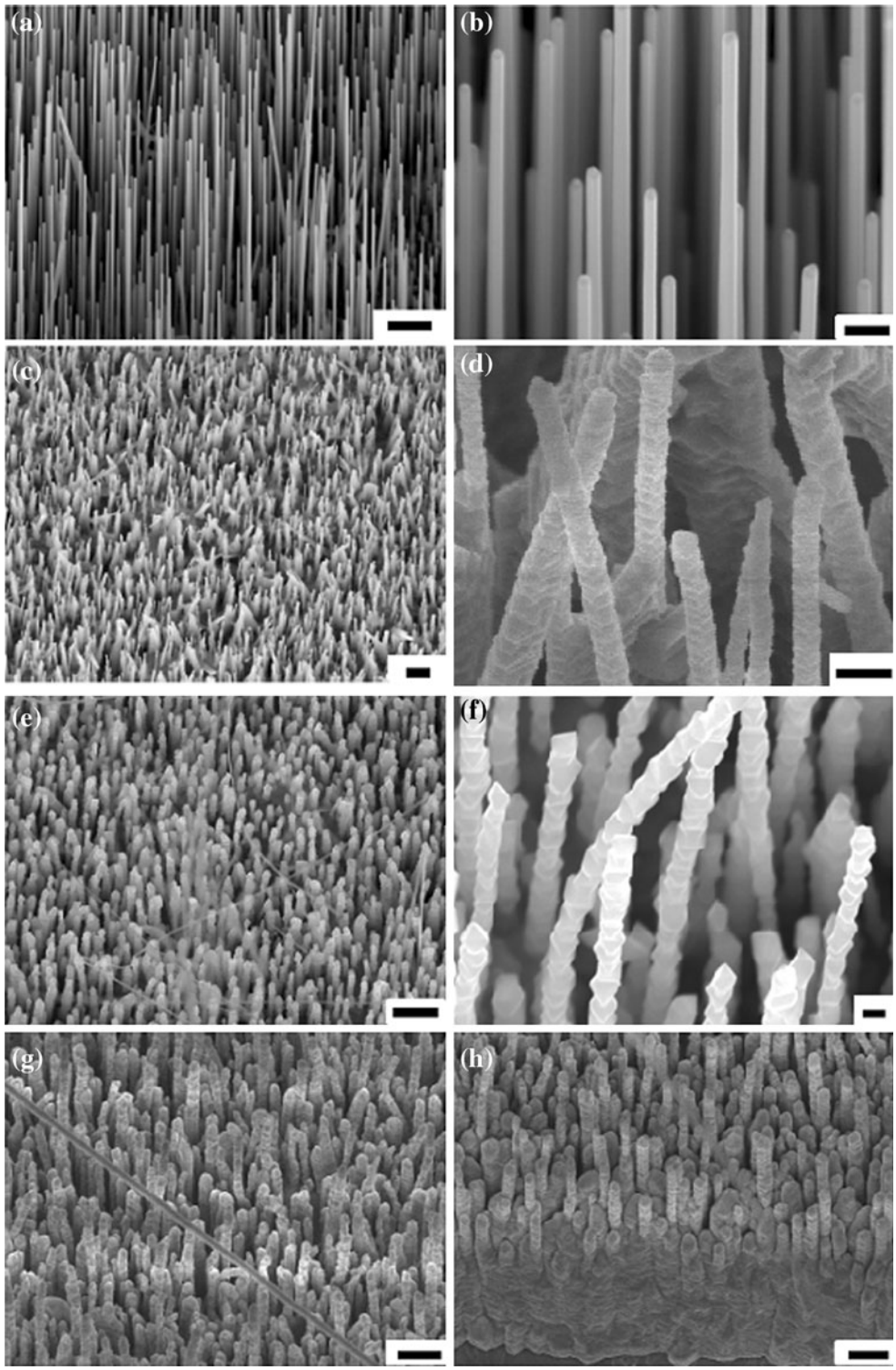
(a)
(b)
(c)
(d)
(e)
(f)
(g)
(h)

◀ **Fig. 2** SEM images of the prepared nanowire samples under low and high magnifications. **a**, **b** Large-scale vertically aligned ZnO nanowires on the *a*-plane sapphire substrate. **c**, **d** Vertically aligned ZnO–ZGO core–shell nanowires synthesized under the ZGO-1 condition of Table 1. **e, f** Vertically aligned ZnO–ZGO core–shell nanowires synthesized under the ZGO-2 condition of Table 1. **g**, **h** Vertically aligned ZnO–ZGO core–shell nanowire grown under the ZGO-3 condition of Table 1. The *scale bars* are 1 μm in **a**, **c**, **e**, **g**, **h** and 200 nm in **b**, **d**, **f**

Table 1 Growth conditions and PL emission peak wavelengths for the three vertically aligned ZnO–$ZnGa_2O_4$ nanowire samples

	ZnO; (Ga_2O_3+C) (g)	Pressure (mbar)	Emissions in PL spectra (nm)
ZGO-1	0; 0.05	40	360, 375, 389
ZGO-2	0.02; 0.05	40	360, 375, 387
ZGO-3	0.05; 0.05	50	360, 376, 386

which is consistent with the value of {111} interplane spacing of the spinel ZGO. The SAED pattern of the core region B (inset B) reveals that the core part of the NW consists of single-crystalline hexagonal ZnO with a [0002] direction parallel to the long-axial direction of the NW. In this case, the calculated interplane spacing between the two close spots in the long-axial direction is ~0.26 nm, which is consistent with the value of {0002} plane spacing of hexagonal ZnO. These two SAED results confirm our XRD analyses of the formation of [111]-oriented ZGO shell layers on [0002]-orientated ZnO NW cores. Furthermore, the SAED pattern of the interfacial region C (inset C) shows two sets of single-crystalline electron diffraction patterns of the spinel ZGO (from ZGO shell area) and the hexagonal ZnO (from ZnO core area). The crystallographic orientations of the ZnO core and the ZGO shell are clearly revealed in the SAED pattern. It is found that the ZGO [111] direction is parallel to the ZnO [0002] direction and the ZGO [2-20] direction is parallel to the ZnO [-2110] direction. Therefore, a parallel relationship between the ZGO (11-2) plane and the ZnO (1–100) plane is predicted. A hetero-epitaxial growth of ZGO shell on ZnO core likely took place to form the ZnO–ZGO core–shell NWs, as shown in Fig. 5.

Usually, spinel ZGO is fabricated through a solid-state diffusion reaction by annealing the two oxyde precursors, β-Ga_2O_3 and ZnO, at a high temperature (above 1,000 °C). In this method, a three-step process

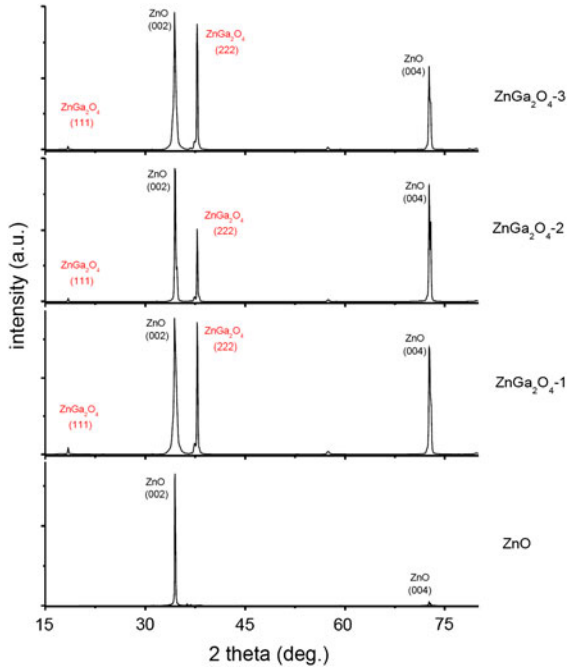

Fig. 3 **a** XRD pattern of the vertical ZnO nanowire sample **b–d** XRD patterns of the ZnO–$ZnGa_2O_4$ nanowire samples prepared under different growth conditions (**b** ZGO-1, **c** ZGO-2, **d** ZGO-3)

is used for the fabrication of core–shell NW structures: a first growth of one precursor oxide AO_x (ZnO or β-Ga_2O_3) NW cores, a second growth of the other precursor oxide BO_x shells surrounding AO_x NW cores, and a final growth of the AO_x-ZGO core–shell NWs by high-temperature annealing (Chang and Wu 2005). However, non-reacted ZnO or β-Ga_2O_3 always remains in the ZGO shell layers using this method. In addition, multiple diffraction peaks of the spinel ZGO phases are usually obtained from the reported XRD patterns, indicating ZGO shells were formed with random crystallographic orientations. In this study, we demonstrated a two-step CVD method for the formation of ZnO–ZGO core–shell NWs with single-crystal quality and well-aligned orientations. In the first step, vertically aligned ZnO NW cores were first fabricated on an *a*-plane sapphire substrate through an Au-catalyzed CVD growth process. Such straight ZnO NWs with smooth sidewall surfaces and an aligned crystal orientation provide a good foundation for the second growth of the radial ZGO shells. In the second CVD step, a vapor-phase diffusion reaction of Ga/O into ZnO NW cores was taken place to directly grow

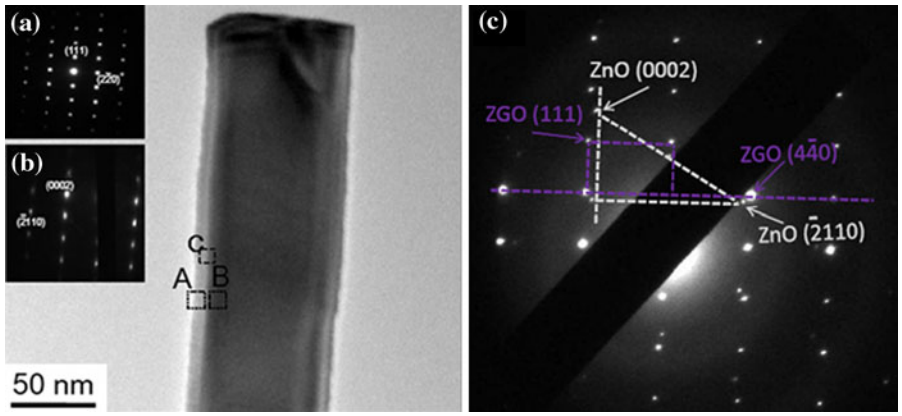

Fig. 4 A bright-field TEM image of an individual ZnO–$ZnGa_2O_4$ core–shell nanowire. Insets are the selected area electron diffraction patterns of the shell (*box A*), the core (*box B*), and interface (*box C*) of the core–shell nanowire

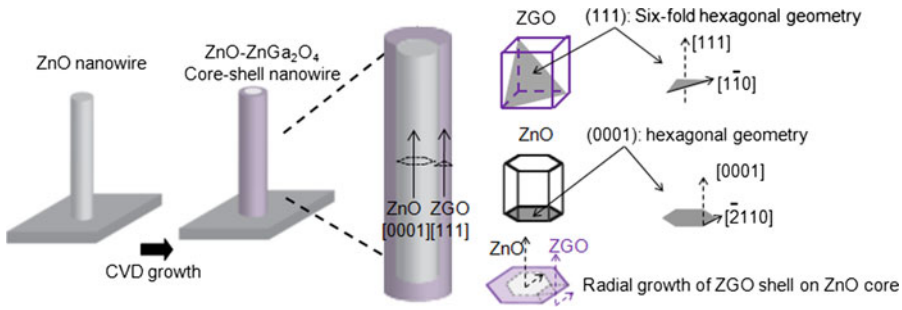

Fig. 5 A schematic of the epitaxial growth of ZnO–$ZnGa_2O_4$ core–shell nanowires and the epitaxial relationship between the $ZnGa_2O_4$ shells and the ZnO cores of the core–shell nanowires

the conformal ZGO NW shells. It is shown that the grown ZGO shells are of single-crystal quality with aligned crystallographic orientation from XRD and TEM analyses.

The growth process of the vertically aligned ZnO–ZGO core–shell NWs is proposed. During the first CVD step, separated Au droplets were likely formed by melting the pre-sputtered discontinuous Au layer at a high-temperature condition. When the vapor sources from the precursors reached the Au droplets, the alloy droplets were formed (Fan et al. 2006; Cao et al. 2011). The alloy kept crystallizing during the CVD growth step to form ZnO nuclei and finally vertical ZnO NWs were formed along the easy growth direction [0001], benefiting from an epitaxial relationship between the ZnO *a*-axis and the *a*-plane sapphire *c*-axis (Yang et al. 2002). Under similar high-temperature growth conditions with our CVD process, Au droplets have been reported to gradually wet the NW sidewalls in a diffusion process and eventually consumed out from the tip area at which time the growth of ZnO NWs is terminated (Hannon et al. 2006). This may be the reason why Au droplets were not found at the tip of NWs. Finally, it should be noted that nanowire growth through a self-catalyzed process cannot be ruled out. After this process, large-scale vertically aligned ZnO NWs were selectively grown on the Au-coated surfaces of the *a*-plane sapphire. In contrast, no ZnO NW was observed on the non-coated substrate area, which indicates that the ZnO nuclei were not easily formed without the assistance of Au under this condition. In the second CVD step, high-temperature vapor-phase deposition reactions were performed to fabricate the ZGO shells. A schematic of the CVD growth of ZGO shells on ZnO cores with an epitaxial relationship between ZGO shells and ZnO cores is shown in Fig. 5. The thickness of the ZGO shells can be tuned by using different amount of precursors and using different growth pressures during the process. When only Ga_2O_3/graphite powder were used as precursors (ZGO-1 condition), the ZGO shells were formed through a diffusion reaction of Ga into ZnO NWs. When a small amount of ZnO powder was added to the Ga_2O_3 precursor in the second CVD step,

thick and non-uniform ZGO layers were formed as shown in the SEM images of the core–shell NWs under the ZGO-2 and ZGO-3 conditions. This is due to a direct chemical deposition of Ga, Zn, and O vapor sources for the formation of ZGO shells, besides the Ga vapor diffusion reactions for the formation of ZGO shells.

The optical properties of the vertically aligned ZnO NWs and the ZnO–ZGO core–shell NWs were investigated. The UV–VIS absorption spectra of the ZnO NWs and the ZnO–ZGO core–shell NWs are shown in Fig. 6. Their corresponding $[F(R)*hv]^{1/2}$ curves are reported in the supplementary material and are used to estimate the band-gap values of ZnO and ZGO. In the UV–VIS absorption spectra, the vertically aligned ZnO NW sample shows one sharp absorption edge with an onset at ~390 nm (corresponding to a band-gap value of 3.2 eV). This is attributed to the near-band-edge absorption of ZnO NWs. In contrast, two clear absorption edges with the onsets at ~295 and ~390 nm were observed in the all three UV–VIS absorption spectra of the ZnO–ZGO core–shell NW samples. The former absorption edge at ~295 nm (corresponding to a band-gap of 4.2 eV) is related to the near-band-edge absorption of the ZGO shells, which is in agreement with the reported band-gap value (around 4.2–4.7 eV) of ZGO (Kumagai et al. 2011). The later absorption edge at ~390 nm has the same value to that of the ZnO NW sample, indicating the near-band-edge absorption of the ZnO cores. It is found that the intensity ratios of the ZGO and ZnO absorption increase in the spectra of the ZGO-2 and ZGO-3 samples, indicating that thicker ZGO shells were formed when ZnO powder was added as a precursor.

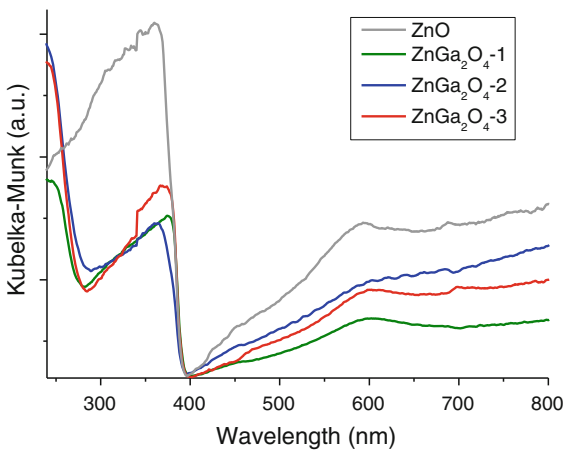

Fig. 6 The UV–VIS diffuse reflectance spectra of the prepared nanowire samples: ZnO nanowire sample (*gray*) and the three ZnO–$ZnGa_2O_4$ core–shell nanowire samples (*green, blue*, and *red*)

The room-temperature PL properties of the vertically aligned ZnO NWs and the ZnO–ZGO core–shell NWs are shown in Fig. 7. In addition, their room-temperature cathodoluminescence spectra were also measured for comparison and are reported in the supplementary material. In the PL spectrum of the ZnO NW sample, one broad visible emission centered at about 500 nm was observed. This broad green emission is known to originate from oxygen vacancies in ZnO (Vanheusden et al. 1996; Wu et al. 2001). The oxygen vacancies are easily formed on the surface and in the bulk of ZnO thin films and NWs during CVD growth process (Soci et al. 2007). In the PL spectra of the three ZnO–ZGO core–shell NW samples, an obvious decrease in the visible emission and a clear increase in the UV emission peaks were observed. The passivation of the broad visible emission is caused by the reduction of oxygen vacancies in ZnO NWs, because the second CVD growth process of the ZnO–ZGO core–shell NWs was conducted in an oxidizing environment under high temperature. The increase in the UV emissions was further investigated. One UV emission peak centered at 360 nm is considered to be from oxygen vacancies in ZGO shells (Kim et al. 2003). It is found that the intensity ratio of this 360 nm peak in the PL spectra increases monotonically from the ZGO-1 sample to the ZGO-3 sample, indicating that thicker ZGO layers were formed when an increased amount of ZnO precursor was used. The UV emission in the range of 370–400 nm is attributed to the ZnO NW cores. Fitting of the UV emission with multiple Gaussians reveals that the broad band UV emission consists of two emission peaks as shown in Fig. 7b. One emission peak centered at ~375 nm (corresponding to a band-gap energy of 3.3 eV) is from the near-band-gap emission of ZnO (or slightly Ga-doped ZnO) (Ye et al. 2005). The other emission peak at ~386–389 nm is red-shifted from the previous ZnO near-band-gap emission peak of ~375 nm and may be interpreted as resulting from donor screening effect in Ga-doped ZnO (Roth et al. 1982, Walsh et al. 2008). The reduced energy of the near-band-gap emission observed in PL spectra follows an empirical relationship (Ye et al. 2005).

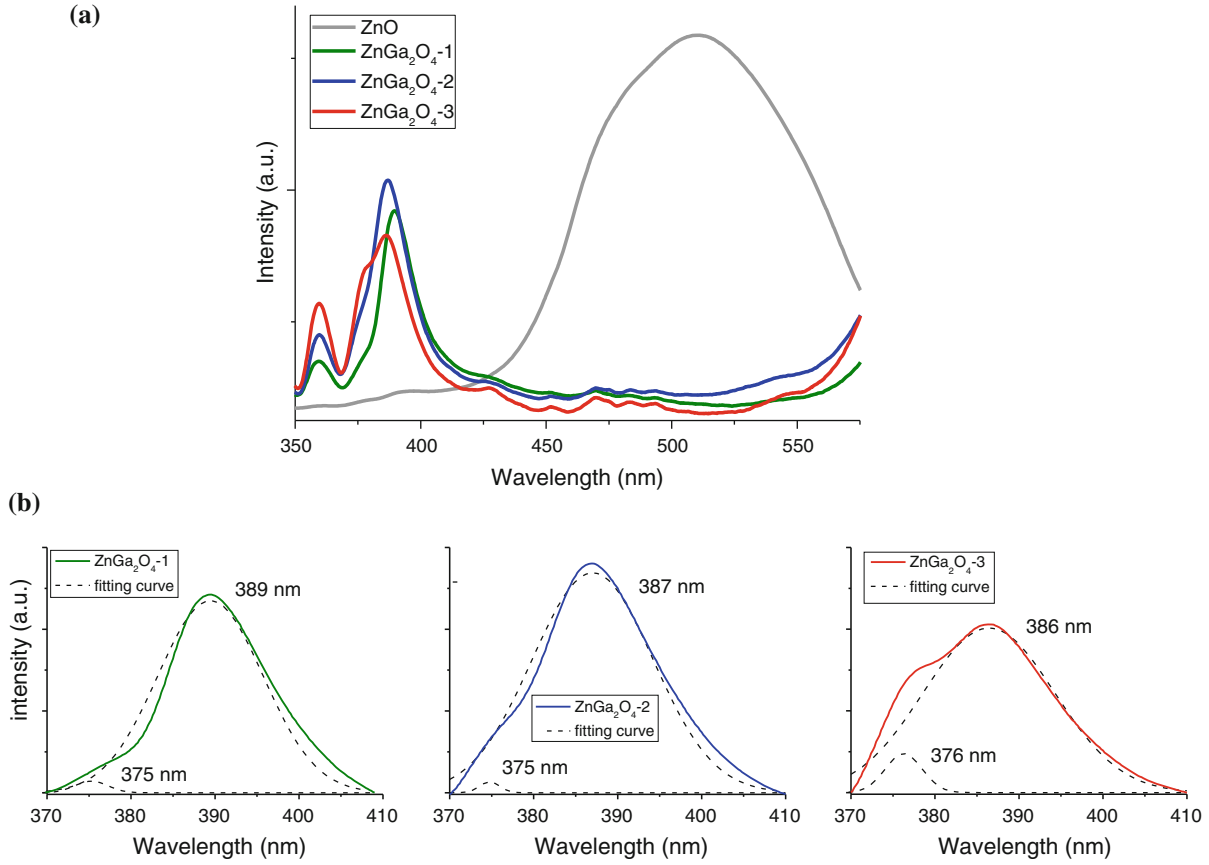

Fig. 7 **a** PL spectra of the prepared nanowire samples: the ZnO nanowire sample (*gray*) and the three ZnO–$ZnGa_2O_4$ core–shell nanowire samples (*green, blue*, and *red*). **b** Gaussian fitting results of the PL emission peaks in the 370–400 nm range of the ZnO–$ZnGa_2O_4$ core–shell nanowire samples

In our study, the ZnO–ZGO core–shell NWs were prepared by a Ga vapor diffusion reaction process, so that the Ga-doped ZnO layers were inevitably formed between the ZGO shells and the ZnO cores (or slightly Ga-doped ZnO cores). Because Ga is a strong donor to ZnO (Yuan et al. 2008), red-shifted near-band-gap emissions of the Ga-doped ZnO layers were observed in the PL spectra. The amount of red shift is related to the Ga-doping concentration in ZnO. We found that a monotonic decrease in the emission wavelength from 389 to 386 nm coincides with the increase in ZnO precursor from 0 to 0.05 g. This is because an increased amount of the ZnO precursor in the second CVD process likely passivates the Ga vapor diffusion reaction, resulting in a decreased Ga-doping concentration in the Ga-doped ZnO layers. From the PL analyses, a three-layer structure of ZnO core, Ga-doped ZnO middle-layer, and ZGO shell was likely formed in the ZnO–ZGO core–shell NWs, as shown in Fig. 8.

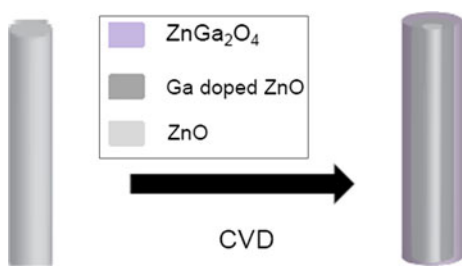

Fig. 8 A proposed three-layer nanowire structure of ZnO core, Ga-doped ZnO middle-layer, and $ZnGa_2O_4$ shell

Conclusions

Dense and large-scale ZnO–ZGO core–shell NWs were synthesized on *a*-plane sapphire substrate by a

simple two-step CVD method. The synthesized ZnO–ZGO core–shell NWs were straightly aligned in high density, with non-uniform shell surfaces and with their roots bonded together on an under-layer of the same material. The ZnO cores and ZGO shells of the core–shell NWs are found to be of single-crystal quality and have aligned crystallographic orientations as evidenced from XRD and TEM analyses. UV–VIS diffuse reflectance spectra of ZnO–ZGO core–shell NWs show two clear near-band-edge absorption of the ZnO cores and the ZGO shells. PL spectra of the ZnO–ZGO core–shell NWs show three UV emission peaks from ZGO shells and ZnO/Ga-doped ZnO cores. We expect that the controllable synthesis of dense and vertically aligned ZnO–ZGO core–shell NWs with promising photoelectric properties will contribute to the development of energy conversion devices such as efficient photoanodes in photoelectrochemical water splitting cells.

Acknowledgements This study was supported through the JSPS program, "Japan Society for the Promotion of Science", Global COE Program, "Global Center of Excellence for Mechanical Systems Innovation," and Grants-in-Aid for Scientific Research (B) 22360056 from the Ministry of Education, Culture, Sports, Science and Technology (MEXT), Japan. The authors thank Prof. Kazunari Domen and Prof. Jun Kubota (Department of Chemical System Engineering, The University of Tokyo) for the UV–VIS diffuse reflectance spectra measurements.

References

Bakkers EPAM, Dam JAV, Franceschi SD, Kouwenhoven LP, Kaiser M, Verheijen M, Wondergem H, Sluis PAD (2004) Epitaxial growth of InP nanowires on germanium. Nat Mater 3:769–773

Cao BB, Chen J, Huang R, Ikuhara Y, Hirayama T, Zhou W (2011) Axial growth of Zn_2GeO_4/ZnO nanowire heterojunction using chemical vapor deposition. J Cryst Growth 316:46–50

Chang K, Wu J (2005) Formation of well-aligned $ZnGa_2O_4$ nanowires from Ga_2O_3/ZnO core-shell nanowires via a Ga_2O_3/$ZnGa_2O_4$ epitaxial relationship. J Phys Chem B 109:13572–13577

Du X, Zhu Y, Yang T, Shen Y, Zeng Y, Xu F (2009) Synthesis and morphology evolution of GaN/C nanocables. J Nanopart Res 11:1179–1183

Fan HJ, Werner P, Zacharias M (2006) Semiconductor nanowires: from self-organization to patterned growth. Small 2:700–717

Fan HJ, Yang Y, Zacharias M (2009) ZnO-based ternary compound nanotubes and nanowires. J Mater Chem 19: 885–900

Han W, Zhang Y, Nam C, Black CT, Mendez EE (2010) Growth and electronic properties of GaN/ZnO solid solution nanowires. Appl Phys Lett 97:083108–083111

Hannon JB, Kodambaka S, Ross FM, Tromp RM (2006) The influence of the surface migration of gold on the growth of silicon nanowires. Nature 440:69–71

Huang YJ, Boukai A, Yang PD (2009) High density *n*-Si/*n*-TiO_2 core/shell nanowire arrays with enhanced photoactivity. Nano Lett 9:410–415

Ikarashi K, Sato J, Kobayashi H, Saito N, Nishiyama H, Inoue Y (2002) Photocatalysis of water decomposition by RuO_2–dispersed $ZnGa_2O_4$ with d^{10} configuration. J Phys Chem B 106:9048–9053

Kim JS, Kang HI, Kim WN, Kim JI, Choi JC, Park HL, Kim GC, Kim TW, Huang YH, Mho SI, Jun MC, Han M (2003) Color variation of $ZnGa_2O_4$ phosphor by reduction-oxidation processes. Appl Phys Lett 82:2029–2031

Kumagai N, Ni L, Irie H (2011) Visible-light-sensitive water-splitting photocatalyst composed of Rh^{3+} in a $4d^6$ electronic configuration, Rh^{3+}-doped $ZnGa_2O_4$. Chem Commun 47:1884–1886

Lauhon LJ, Gudiksen MS, Wang D, Lieber CM (2002) Epitaxial core-shell and core-multishell nanowire heterostructures. Nature 420:57–61

Li YJ, Lu Y, Wang CW, Li KM, Chen LJ (2006) $ZnGa_2O_4$ nanotubes with sharp cathodoluminescence peak. Appl Phys Lett 88(143102):1–3

Maeda K, Takata T, Hara M, Saito N, Inoue Y, Kobayashi H, Momen K (2005) GaN:ZnO solid solution as a photocatalyst for visible-light-driven overall water splitting. J Am Chem Soc 127:8286–8287

Roth AP, Webb JB, Williams DF (1982) Band-gap narrowing in heavily defect-doped ZnO. Phys Rev B 25:7836–7839

Shu Q, Wei J, Wang K, Zhu H, Li Z, Jia Y, Gui X, Guo N, Li X, Ma C, Wu D (2009) Hybrid heterojunction and photoelectrochemistry solar cell based on silicon nanowires and double-walled carbon nanotubes. Nano Lett 9:4338–4342

Soci C, Zhang A, Xiang B, Dayeh SA, Aplin DPR, Park J, Bao XY, Lo YH, Wang D (2007) ZnO nanowire UV photodetectors with high internal gain. Nano Lett 7:1003–1009

Thelander C, Agarwal P, Brongersma S, Eymery J, Feiner LF, Forchel A, Scheffler M, Riess W, Ohlsson BJ, Gosele U, Samuelson L (2006) Nanowire-based one-dimensional electronics. Mater Today 9:28–35

Vanheusden K, Warren WL, Seager CH, Tellant DR, Voigt JA, Gnade BE (1996) Mechanisms behind green photoluminescence in ZnO phosphor powders. J Appl Phys 79:7983–7990

Walsh A, Silva JLFD, Wei S (2008) Origins of band-gap renormalization in degenerately doped semiconductors. Phys Rev B 78:075211 1–075211 5

Wang K, Chen J, Zhou W, Zhang Y, Yan Y, Pern J, Mascarenhas A (2008) Direct growth of highly mismatched type II ZnO/ZnSe core/shell nanowire arrays on transparent conducting oxide substrates for solar cell applications. Adv Mater 20:3248–3253

Wu XL, Siu GG, Fu CL, Ong HC (2001) Photoluminescence and cathodoluminescence studies of stoichiometric and oxygen-deficient ZnO films. Appl Phys Lett 78:2285–2287

Yang PD, Yan HQ, Mao S, Russo R, Johnson J, Saykally R, Morris N, Pham J, He R, Choi H (2002) Controlled growth

of ZnO nanowires and their optical properties. Adv Funct Mater 12:313–323

Ye JD, Gu SL, Zhu SM, Liu SM, Zheng YD, Zhang R, Shi Y (2005) Fermi-level band filling and band-gap renormalization in Ga-doped ZnO. Appl Phys Lett 86:192111–192114

Yuan G, Zhang W, Jie J, Fan X, Tang J, Shafiq I, Ye Z, Lee C, Lee S (2008) Tunable n-type conductivity and transport properties of Ga-doped ZnO nanowire arrays. Adv Mater 20:168–173

Zhong M, Li Y, Yamada I, Delaunay J–J (2012) ZnO-$ZnGa_2O_4$ core-shell nanowire array for stable photoelectrochemical water splitting. Nanoscale 4:1509–1514